Synthetic Aperture Radar Simulation for Point and Extended Targets

SYNTHETIC APERTURE RADAR SIMULATION FOR POINT AND EXTENDED TARGETS

BY

AKINTUNDE ADEWOYE,

A THESIS

SUBMITTED TO THE DEPARTMENT OF ELECTRICAL & COMPUTER ENGINEERING

AND THE SCHOOL OF GRADUATE STUDIES

OF MCMASTER UNIVERSITY

IN PARTIAL FULFILMENT OF THE REQUIREMENTS

FOR THE DEGREE OF

MASTER OF APPLIED SCIENCE

Master of Applied Science (2013) McMaster University

(Electrical & Computer Engineering) Hamilton, Ontario, Canada

TITLE:	Synthetic Aperture Radar Simulation for Point and Extended Targets
AUTHOR:	Akintunde Adewoye B.Eng., (Electrical Engineering) McMaster University, Hamilton, ON, Canada
SUPERVISOR:	Dr. Thia Kirubarajan
NUMBER OF PAGES:	xii, 52

This thesis is dedicated to my parents

Abstract

Basic radar systems use electromagnetic wave reflections from targets to determine the motion characteristics of these targets. Synthetic Aperture Radar (SAR) systems use the reflections to produce target images as well. SAR is an imaging radar system that produces high resolution images of a scene or target by using radar motion to synthesize the antenna aperture. A SAR model to handle extended targets and point targets in faster time is presented, as are some simulated results.

This thesis explains synthetic aperture concepts, the model used and a simulation of a SAR system. It runs through modelling point targets as well as extended targets by using the resolution cells of the radar, creating the raw signal data from the target information and then the signal processing that converts the raw data to a SAR image. The simulation was done for better understanding of synthetic aperture parameters and it was done in C++ programming language for improved processing speed.

In comparison to previous simulations obtained from literature review, there is an increase in speed of more than 2.5 times as the number of targets increases, producing higher resolution images in less time. A model to handle extended targets was presented while also showing the imperfections due to the model assumptions. These assumptions are then explained as the best option in the absence of extra geographic information on the target scene.

Acknowledgements

I would like to thank Dr. T. Kiruba for his guidance and supervision and also for giving me the privilege to work with him and other great people through the entirety of my program. I am grateful to Dr. Ali Gorji, Dr. Tharmas and Biruk for their willingness to answer my questions and help throughout the course of this project.

A big thank you goes to my parents and sisters - Anu and Ore, who have supported me with their all, throughout all phases of my education and helped me to this point in my life. I also appreciate the efforts of my best friend, Zino who has been nothing but supportive and encouraging since the beginning.

Most importantly, I would like to thank God; none of this would be possible without Him!

Notation and abbreviations

Abbreviations

The abbreviations used in this thesis are listed below

RADAR	-	Radio Detection and Ranging
SAR	-	Synthetic Aperture Radar
RDA	-	Range Doppler Algorithm
PRF	-	Pulse Repetition Frequency
BW	-	Bandwidth
EM	-	Electromagnetic
2-D	-	Two-dimension(al)
3-D	-	Three-dimension(al)
FT	-	Fourier Transform
FFT	-	Fast Fourier Transform
IFFT	-	Inverse Fast Fourier Transform
CSA	-	Chirp Scaling Algorithm
Open CV	-	Open source Computer Vision

Interchangeable terms

The following terms are used interchangeably throughout the course of this thesis.

Range time	-	Fast time
Azimuth time	-	Slow time
Spotlight SAR	-	Spot SAR
Azimuth sampling rate	-	PRF
Target	-	Scatterer
Radar	-	Sensor

Note : In this paper, the term scene was mostly used to describe targets due to limited motion of targets considered. To refer to targets which were in some kind of motion, the term 'moving targets' was used.

Notations

c	-	speed of light
τ	-	range time
η	-	azimuth time
λ	-	wavelength
ρ	-	resolution
ρ_a	-	azimuth resolution
ρ_r	-	range resolution
L_a	-	antenna length
L_s	-	synthetic aperture length
K_a	-	range FM rate
K_r	-	azimuth FM rate
T_r	-	pulse duration/period
T_x	-	Transmitted wave
R_x	-	Reflected/received wave
V_r	-	platform/radar velocity
f_0	-	centre frequency
$R(\eta)$	-	slant range
$w(.)$	-	window [rectangular or sinc]
$s(\tau, \eta)$	-	raw SAR data
A'	-	cross-sectional area
A	-	reflectivity

Contents

List of Figures

Chapter 1

INTRODUCTION AND PROBLEM DEFINITION

This chapter provides an introduction on Synthetic Aperture Radars (SAR), briefly introduces its concepts, explains how SAR works and its purpose and advantages over basic radars. This chapter also describes the motivation for this project, previous work done on SAR and the contributions made in this paper.

1.1 Introduction

Synthetic Aperture Radar (SAR) is a type of radar that uses the relative motion between a target and a sensor, which is usually placed on a platform, to produce two dimensional high resolution images of that target. This relative motion could be achieved in two major ways: a stationary target and a moving sensor or a moving target and a stationary sensor; the latter describes a form of SAR called Inverse Synthetic Aperture Radar (ISAR). Newer algorithms are being developed to handle cases

of a moving target and a moving sensor with some including the use of Kalman filters [3, 4, 5]. The basic concept of SAR is to use signal processing to generate the result of a longer antenna. Radar operations involve the transmission of electromagnetic waves toward an object, the reception of the reflected waves by this object and the calculation of certain motion characteristics of the target under consideration from the properties of reflected waves and the time taken to receive it. In the case of SAR, the EM waves used are referred to as a beam, which is produced from an aperture. The smaller the aperture length, the wider the beam width, which could be explained by the phenomenon of diffraction. It will be seen later on that the wider the beam width, the higher the resolution, but the aperture cannot be made infinitely small because the SNR is directly proportional to the beam width. The synthetic aperture process involves a radar mounted on a moving platform, sending down a beam toward (or illuminating) the surface of the earth. The reflections from this beam are then recorded and later processed. This paper proposes a model with a refined target input structure and processes the reflections from targets in faster time than older models. Synthetic aperture radars have three main modes of operation: strip-map SAR, spotlight SAR and Scan SAR. The strip-map mode, as shown in Figure 1.1, is a mode of SAR operation where the radar beam illuminates the part of the ground along which the platform is travelling i.e., the censored area is parallel to the motion of the platform. This is also referred to as side-looking SAR or strip SAR [6]. In the spotlight mode of operation, the beam is focused on a particular region of the ground of area of interest throughout the entire motion of the platform. This can be seen in Figure 1.2. For the scan SAR mode, the target scene is divided into several segments; as the radar platform moves, the radar illuminates one segment for a period of time,

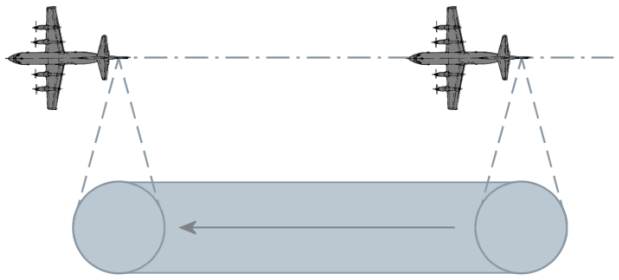

Figure 1.1: Strip-map SAR mode of operation

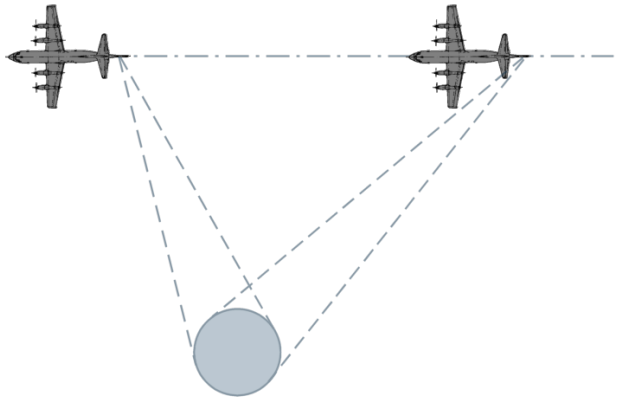

Figure 1.2: Spotlight SAR mode of operation

then switches to illuminate another segment [6].

Figures 1.1, 1.2 and 1.3 also serve the purpose of visually describing the operation of synthetic aperture radars, as well as showing the different ways in which they could operate. All three modes include the motion of the radar platform but differ in the pattern of this motion; each of which have different uses too. Although other variations of SAR exist such as the afore mentioned ISAR and interferometric SAR, these are the major modes of operation.

A SAR system works fine even in dark environments because it produces its own illumination. Its use of light waves makes the radar independent of its surrounding

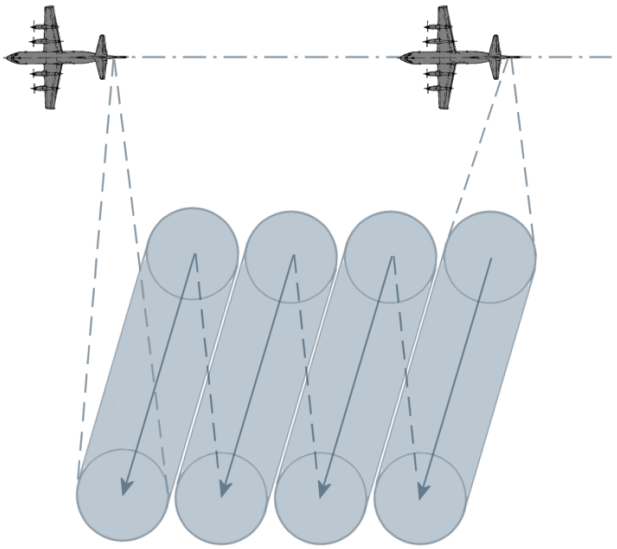

Figure 1.3: Scan SAR mode of operation

or an external lighting system. Also, it is able to work through cloudy environments because of the longer wavelength of the radar in comparison to visible light hence, reducing the scattering effect of clouds, leaving the reflected wave relatively undistorted [7, 1]. Common applications of SAR include surveillance, change detection as in the case of interferometric SAR, land cover mapping, monitoring flood, forest fires, sea ice, volcanic eruptions, oil spills, detection of ships, land vehicles and other ground targets [7, 1]. Synthetic aperture radars have high resolution in range and azimuth due to pulse compression which involves phase modulation, and further down the process, matched filtering. Matched filtering on a complex-valued signal is the application/correlation of a time-reversed complex conjugate of that signal on itself to maximize SNR; this is sometimes referred to as template matching [8]. The added noise to the signal is assumed to have a flat power spectral density. The modulation in range is carried out by using a chirp pulse while the modulation in azimuth

comes about due to the motion of the platform. This is explained in more detail in Chapter 2.

1.2 Literature review

The books "Synthetic Aperture Radar Signal Processing with MATLAB Algorithms" by Mehrdad Soumekh, "Digital processing of synthetic aperture radar data" by Cumming and Wong [1], and the dissertation "Synthetic Aperture Radar Imaging Simulated in Matlab" by Matthew Schlutz in 2009 were used as a starting point at the beginning of this project in 2012. Also reviewed was a thesis "High Resolution Simulation of Synthetic Aperture Radar Imaging" by Cindy Romero [9]. Although the ultimate goal of Schlutz's project was Automatic Target Recognition, this was a good starting point as it was useful to see what already exists and improve on it. The work done by Schlutz was an enhancement of work done by previous students in the California Polytechnic lab; his simulation took in an image as the input to model the scene and each pixel was treated as point target with the pixel value representing the reflectivity. The reflections from each target were modelled and then these data was processed by an algorithm called RDA into a SAR image. Due to the number of reflections from each target, the number of pixels that could be processed was very limited as a result of the processing time. Cindy Romero, in her thesis, replaced this input model with images generated by blender and she also re-modelled the reflections by introducing Quadrature Demodulation Signature to save processing time, as this was the most time consuming section of the simulation. The aforementioned books modelled SAR systems for point targets, including multiple processing algorithms for SAR data, some of which were extracted for use in the simulation [1].

1.3 Motivation and Contributions of this thesis

1.3.1 Motivation

The ultimate aim of this simulation is to enhance target tracking and detection. Multiple tracking systems and radar simulations of high quality have been developed by previous students and researchers in the Estimation, Tracking and Fusion laboratory at McMaster University supervised by Dr. Thia Kiruba. This is an enhancement of the radar systems library that would be used for tracking targets eventually. This is the first SAR simulation to be done in this lab. This model could also be useful for Automatic Target Recognition (ATR) systems as shown in the previous section.

1.3.2 Contributions

This thesis has two major contributions. These include target modelling and an attempt to increase the simulation speed with regards to previous simulations. From the literature review done, Matthew Schlutz's work used an image to describe the target profile. It is assumed that this is due to the fact that the main goal of his project is ATR since it will be convenient to test and compare results obtained from the radar. The purpose of this simulation is to track a particular target of interest. Therefore, an image of the target would not be appropriate since further work could see tracking algorithms added to this simulation to help track and detect certain moving and/or stationary targets in a scene of interest. In reality, the image (or imaging information) of the scene is usually not available before SAR imagery and more importantly, there is a chance that multiple pixels fall in one resolution cell if pixels are treated as point targets. Due to this, a different model had to be used for

the target profile than that used in the paper stated above. The new model allowed for point targets and a general model for certain extended targets of interest in a scene, which includes discretization of extended targets using the resolution cells of the radar. This model is explained in further detail in Chapter 3.

Also, due to the processing time of generating reflections from the targets, the processing time needed to be improved to allow a larger number of (point) targets and in doing so, higher resolution images. Therefore, this simulation has been done in C++ programming language with the aid of OpenCV library to handle images and signal processing needed during the simulation. Other changes include the raw data generation and the signal processing of the resulting data into an image.

1.4 Thesis Organization

The current chapter has introduced the concepts of SAR, current and possible applications, explained the literature review done and stated the motivation as well as the major contributions of the thesis. The subsequent chapters will drive toward modelling of the radar and target. The synthetic aperture radar concepts briefly introduced earlier in this chapter will be explained in more detail in Chapter 2 with an insight to understanding the model. In Chapter 3, the radar model is described starting with how the target was modelled, which is one of the major parts of the thesis. The assumptions made during the simulation are also discussed here. The results of the simulation are presented in Chapter 4, and Chapter 5 will conclude the thesis with recommendations and areas for future work. This is followed by the appendix, which describes the software (programming language and libraries) used and briefly explains the flow of the SAR simulator. The references used throughout

writing the paper, target and radar modelling as well as simulations bring the thesis to conclusion.

Chapter 2

SAR CONCEPTS

A radar placed on a platform, which is moving at constant velocity, is transported over a certain distance known as the synthetic aperture length as shown in Figure 2.1. This can be also described as the distance the sensor travels while the target is illuminated by the radar beam. At sampled times during the flight, the radar is transmitting pulses toward a target or targets in the area of interest and receives the reflections from these targets. Every received reflection during the flight is stored in memory, the array of these saved reflections are referred to as raw SAR data. After the raw data is collected, it then passes through signal processing steps that focus these targets to produce a high resolution image of the area of interest. This, as shown in Figure 2.2 describes the mode of operation of a synthetic aperture radar. Consequent sections in this chapter will explain the raw data collection and processing as a two dimensional problem, which includes the transmission and reception of EM waves, and also the processing steps involved to transform raw SAR data to an image.

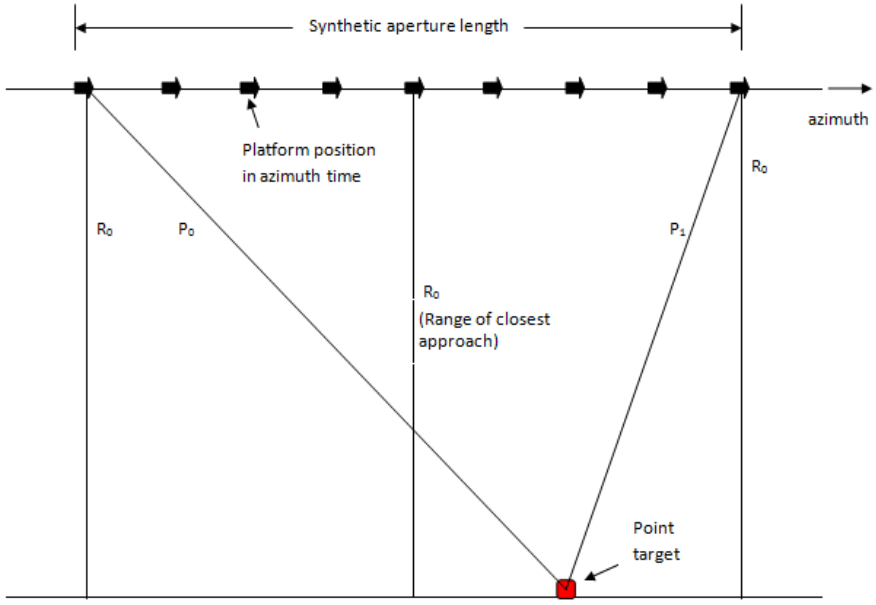

Figure 2.1: Synthetic aperture length

2.1 SAR as a 2D problem

The output SAR signal (often referred to as raw SAR data) before signal processing, can be interpreted as a two dimensional signal. These dimensions include the fast time, which refers to range direction and the slow time, which is the azimuth direction. Picture a scenario with a simple stationary sensor and a point scatterer; when an EM wave, which is a function of time, say $T_x(\tau)$, is transmitted from the sensor's transmitter to the scatterer, the wave at the sensors receiver is a scaled and shifted version of the original wave, $R_x(\tau) = \mathrm{A}T_x(\tau - \tau_0)$. Now assume this function $R_x(\tau)$ is also a function of another variable say η, this results in a function $R_x(\tau, \eta)$. In the SAR case, the variable η is defined as the azimuth time or slow time, and is controlled by the motion of the platform. The azimuth direction is defined as the direction parallel

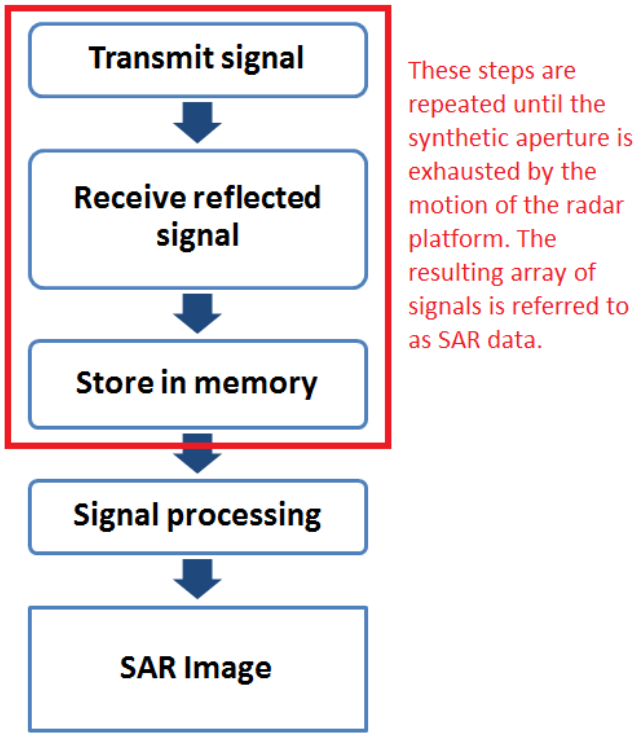

Figure 2.2: SAR process

to the relative motion of the platform. Figure 2.3 shows how this data is collected and illustrates the collected data in both dimensions, which are explained below.

2.1.1 Range direction (Fast time)

At a particular point in time, the transmitter sends out a series of pulses, and the sensor's receiver gets reflections shortly after. Note that this does not occur at the same point in time, but by comparing the speed of light, the distance between the target and radar, and the speed at which the platform is moving, it is a fair approximation that the wave was sent out and received at the same time [1]. The transmitted pulse

figure 2.3a figure 2.3b

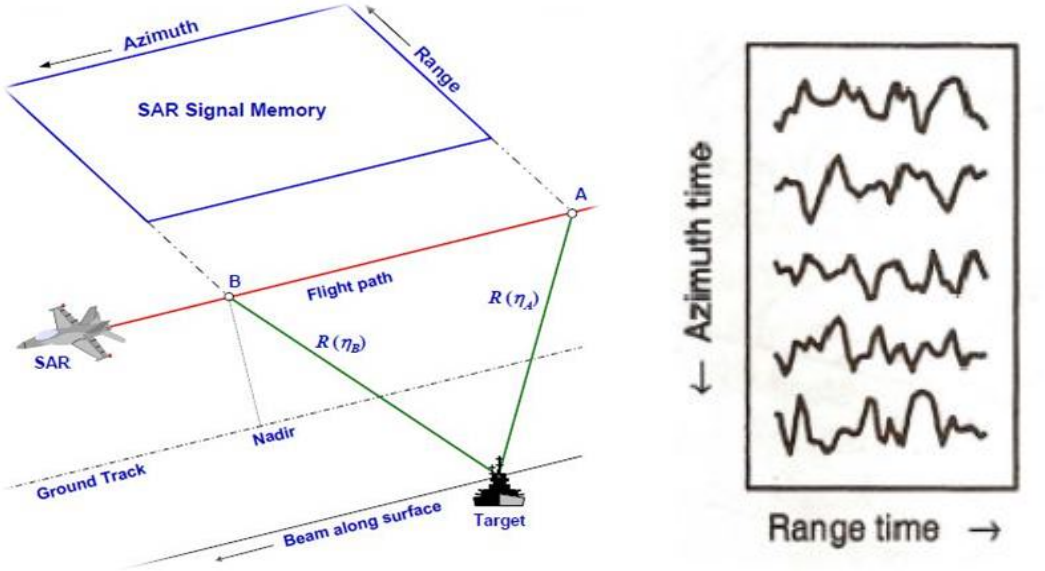

Figure 2.3: SAR as a two dimensional problem

sent out by the radar is an FM pulse represented by

$$s_{pul}(\tau) = w_r(\tau)\exp(j2\pi f_i\tau) \tag{2.1}$$

or the real part

$$s_{pul,re}(\tau) = w_r(\tau)\cos(2\pi f_i\tau) \tag{2.2}$$

where

$f_i = f_0 + K_r\tau$ is the instantaneous frequency

τ = range time, referenced to the centre of the pulse

$w_r(\tau)$ = the pulse envelope, a rectangular function with a pulse duration of T_r

That is, $w_r(\tau) = \text{rect}(\frac{\tau}{T_r})$

K_r = FM rate of the range pulse

A positive sign of K_r represents an up-chirp while a negative sign represents a down-chirp.

Equation 2.1 shows that the wavelength of the pulse, which is c/f_i, also varies within the pulse; however, this variation in wavelength is not obvious after demodulation, hence the definition of λ used is c/f_0. To avoid aliasing problems, the demodulated received signal must be sampled with a rate, F_r, that should be higher than the pulse bandwidth, which is given by $|K_r|T_r$ [1]. According to the Nyquist criterion, the sampling rate must be a least twice the pulse bandwidth.

After transmission, the pulse received by the sensor from a point reflector that is R_a meters away will be a scaled and shifted version of the original pulse, which could be represented by

$$s_{rec}(\tau) = \mathrm{A}s_{pul}(\tau - \frac{2R_a}{c}) \tag{2.3}$$

$$s_{rec}(\tau) = \mathrm{A}w_r(\tau - \frac{2R_a}{c})\cos(2\pi f_i(\tau - \frac{2R_a}{c})) \tag{2.4}$$

where f_i is now $f_0 + K_r(\tau - 2R_a/c)$ and A represents the scale/reflectivity of the target.

An important quality/performance evaluator of radars is the resolution. This is defined as the ability of the radar to differentiate between two targets that are closely located either in range or azimuth. Generally, in the case of a simple radar, transmitting a pulse, $p(t)$, with a width of T, the range resolution is

$$\rho_r = \frac{c \times T}{2} \text{ (where c = speed of light)}. \tag{2.5}$$

The energy from the signal, $p(t)$ is

$$E = \int_0^T |p(t)|^2 \, dt \tag{2.6}$$

which yields $E = A_{pulse}^2 T$, if A_{pulse} is the pulse amplitude. From (2.5), ρ_r gets smaller, that is, the resolution increases and improves as the pulse width reduces. While a relatively low number is desired for a radar system, it comes at the expense of the signal-to-noise ratio (SNR), which as seen in (2.6) increases as the pulse width increases. This problem can be solved by the use of pulse compression [6]. This technique consists of modulating the pulse, then performing matched filtering after the pulse is received. Due to pulse compression in the case of SAR, a high range resolution can be achieved. After pulse compression, the carrier wave has a much larger bandwidth, then the range resolution, ρ_r, obtained expressed in time units is

$$\rho_r = \frac{0.866}{|K_r|T_r} \tag{2.7}$$

and in slant range (distance) units,

$$\rho_r = \frac{0.866c}{2|K_r|T_r} \tag{2.8}$$

Range resolution $\rho_r \approx \frac{c}{2|K_r|T_r}$ after applying a window and could be in the range of centimetres due to this 'new' bandwidth [1].

2.1.2 Azimuth direction (Slow time)

As explained in the previous section, the radar sends out an FM pulse modelled by (2.3) and the second dimension in the SAR signal comes about due to the motion of the platform. Consider (2.4), now R_a is a function of the motion of the platform (that is, the slant range between the radar, and the target changes as the platform moves). From (2.4), R_a now becomes dependent on slow time variable η, therefore, R_a can be replaced with R_η. As mentioned earlier, the major property of a synthetic aperture radar is the motion of the platform. As seen in Figure 2.1 or 2.3(a), the distance from point P_0 [or $R(\eta_B)$] to the target, and point P_1[or $R(\eta_A)$] to the target is different. These distances are referred to as slant range. The slant range from Figure 2.4 changes as the platform moves (that is, the azimuth time changes). The motion of the platform has two major implications, the first of which is a phase modulation from pulse to pulse, and also range cell migration (RCM) due to one target showing up at multiple resolution cells during the duration of the platform motion [1]. Later in this section, it will be shown how the phase modulation enhances the azimuth resolution; in the next section, the effect of RCM is described further and so is how it is handled/corrected. The slant range at a particular point in azimuth time can be modelled using the Pythagorean theorem, which is seen in Figure 2.4.

$$R(\eta)^2 = R_0^2 + X^2 \tag{2.9}$$

Under the assumptions that the flight path is locally straight, the earth is locally flat; it has a small curvature. This case assumes the platform is an aircraft, therefore the speed of the aircraft also equals the progression of the beam footprint along the

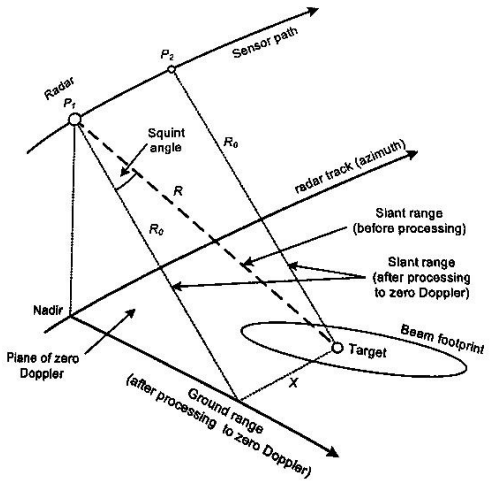

Figure 2.4: SAR slant range

surface. Another assumption in the slant range model is that the target is stationary or has limited mobility with a known motion model. $X = V_r\eta$ is the distance travelled from point 1 to point 2, which is simply the platform velocity multiplied by the (azimuth) time taken to travel between both points. R_0 is the slant range when radar is closest to the target (range of closest approach). After demodulation, the received signal is of the form [1]

$$s(\tau,\eta) = \mathrm{A}w_r(\tau - \frac{2R(\eta)}{c})w_a(\eta-\eta_c) \times \exp(-j4\pi f_0\frac{R(\eta)}{c}) \times \exp\{j\pi K_r(\tau - \frac{2R(\eta)}{c})^2\} \tag{2.10}$$

where η_c is the beam centre crossing time and w_a is the azimuth window. The azimuth window is applied as a result of varying signal strength due to the beam pattern. The maximum signal strength is received when the radar is placed directly over the target, i.e., when slant range is minimum (range of closest approach). As the radar either approaches or moves away from this point, the target is no longer illuminated fully by

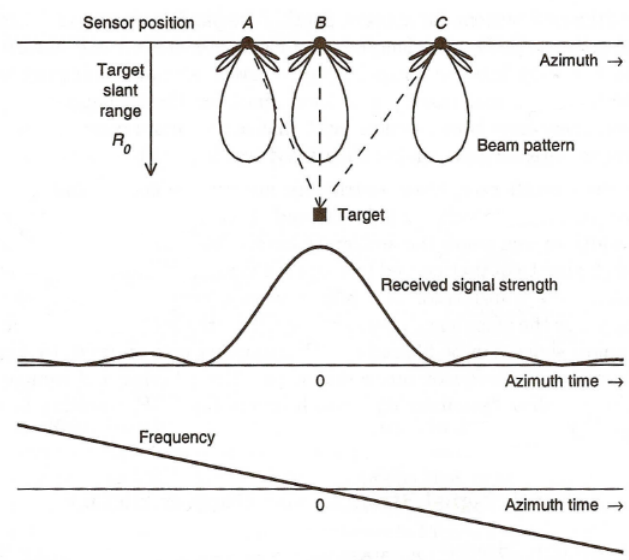

Figure 2.5: Effect of platform motion on signal strength[1]

the radar pulse hence the strength of the received signal is lower. This can be clearly seen in Figure 2.5. The beam pattern is approximated in the book by Cumming and Wong [1] as

$$p_a(\theta) \approx \text{sinc}(\frac{0.886\theta}{\beta_{bw}}) \tag{2.11}$$

where θ is the angle the slant range makes with the range of closest approach, $\beta_{bw} = 0.886\lambda/L_a$, represents the azimuth bandwidth and L_a is the length of the antenna. The received signal is represented by the square of the beam pattern, $w_a = p_a^2(\theta)$; note that θ varies as the platform moves, hence it is a function of, η, azimuth time [1].It is also important to note that,there is an effect of attenuation for media with losses. This received data right before the signal processing stage is continuous in range time domain but already sampled in the slow time domain due to the transmit and receive times of the sensor. Although, in this case, the use of a monostatic radar is assumed (i.e., the transmitter and receiver are located in the same position or relatively close),

when the sensor transmitter is transmitting pulses, the receiver is not active. Systems that use separate transmitter and receivers have to ensure this in order to avoid a faulty radar system, i.e., receiving unreflected pulses. A transceiver could be used to achieve this purpose [10].

Generally, the azimuth resolution of a radar is dependent on the beam width in the sense that if two targets are located in the beam width then it is difficult to tell the difference between them from the reflection obtained. For the synthetic aperture radar, just like in the range direction, there is a phase modulation in the azimuth direction but this is due to the motion of the platform. To improve the resolution, the principle of pulse compression could also be applied. Since modulation has already been done as a result of the platform motion, a matched filter will be applied in the azimuth direction to complete the application of pulse compression (pulse compression involves modulation and matched filtering). As mentioned earlier, this technique increases the resolution. A question raised is how does the platform motion phase modulate the SAR signal in the azimuth direction? A more detailed explanation of this concept can be seen in Section 3.3. Using a similar idea to that used in the range direction, the azimuth resolution is the inverse of the bandwidth multiplied by 0.866, $\rho_a = \frac{0.866}{\mathrm{BW_a}}$ where the azimuth bandwidth is represented by $\mathrm{BW_a}$. In distance units this is multiplied by the speed with which the beam moves on the ground and the squint angle at the beam centre. This results in

$$\rho_a = \frac{0.866 V_g \cos\theta_{r,c}}{\mathrm{BW_a}} \tag{2.12}$$

According to Cumming and Wong [1], $\mathrm{BW_a}$, the azimuth bandwidth is given as

$$\mathrm{BW_a} = 0.866\frac{2V_s \cos\theta_{r,c}}{L_a} \tag{2.13}$$

The azimuth resolution calculated here is indeed the cross range resolution but since low squint is assumed, the cross range and azimuth vectors are assumed parallel; the cross range vector is the direction perpendicular to that of the radar's line of sight [1].

The resulting azimuth resolution of the SAR system is given by [1]

$$\rho_a = \frac{L_a}{2} \tag{2.14}$$

where L_a is the antenna length in the azimuth direction.

Figure 2.6 shows the locus of energy in memory for a point target, supplementing Figure 2.3a & Figure 2.3b. This shows a discrete form of Figure 2.3b but also factors the platform motion's change in fast time. This is the cause of range cell migration and the purpose of SAR signal processing is to focus the energy to a point. This will be explained in more detail in the section below.

2.2 Signal Processing of SAR Data

The synthetic aperture radar differs from a basic radar system in two important ways. The first, which is explained in the first section of this chapter, is the motion of the radar/platform on which it is placed; the second is the signal processing involved to transform the received data into an image. As explained in the previous section, the

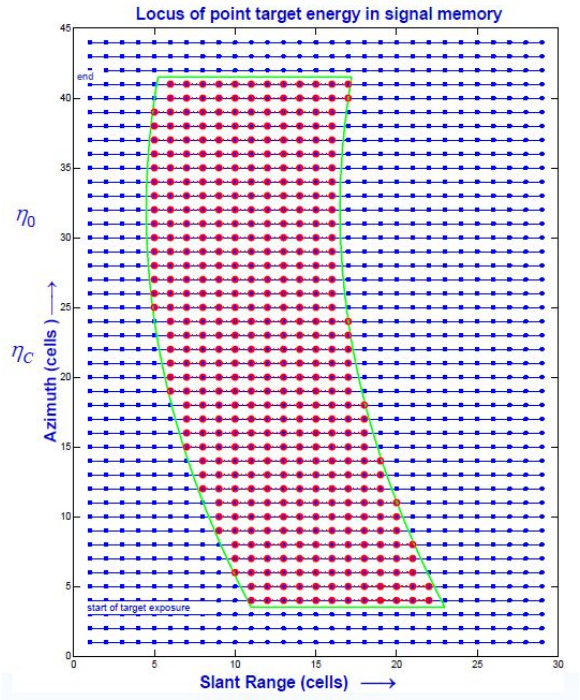

Figure 2.6: Locus of point target energy in memory [2]

SAR data obtained is a two dimensional function dependent on range and azimuth time. Signal processing helps focus the energy of each point target (which as described above is spread across the signal memory in range and azimuth) into single points or pixels on the SAR output image [11]. This is shown in Figure 2.6. According to [1], the main purpose of SAR processing is to determine the ground reflectivity from the convolution problem given below

$$S_{bb}(\tau, \eta) = g(\tau, \eta) * h_{\text{imp}}(\tau, \eta) \tag{2.15}$$

where S_{bb} is the recorded baseband signal, h_{imp} is the impulse response on a unity point target at a particular point in fast time, τ, and slow time, η; $g(\tau, \eta)$ is the ground reflectivity [1]. Due to the time domain convolution in the problem, to improve the

efficiency (simplicity and speed) of SAR processing, most algorithms convert the time domain signal to a frequency domain signal by the use of Fourier transform since convolution in the time domain becomes multiplication in the frequency domain [12, 13, 1]. The most common SAR processing algorithm is described below; several others are also briefly introduced or mentioned in a later section.

2.2.1 Range Doppler Algorithm (RDA)

The range Doppler algorithm is one of the techniques used in transforming raw SAR data from the previous steps into a more useful SAR image. It was used in creating the first digitally processed spaceborne SAR data; it is still widely used today and also considered highly precise and the most efficient SAR processing algorithm [11, 1, 14]. The simplicity of RDA comes from the fact that the dimensions of the raw data are separable due to the large difference in time scales; azimuth time being in the range of hundreds of m/s and range time in the range of the speed of light ($3 \times 10^8 \frac{m}{s}$) [1]. This algorithm involves several steps, which can be seen in Figure 2.7; range compression, azimuth FFT, RCMC, azimuth compression and azimuth IFFT. These steps are explained in more detail below.

Range compression

Range compression consists of 3 steps: performing range Fourier transform, followed by applying matched filtering, i.e., multiplying the received data with the time-reversed complex conjugate of a range signal template (in the frequency domain), and then a range inverse Fourier transform. This completes the range pulse compression, which was introduced earlier by modulating the range time signal.

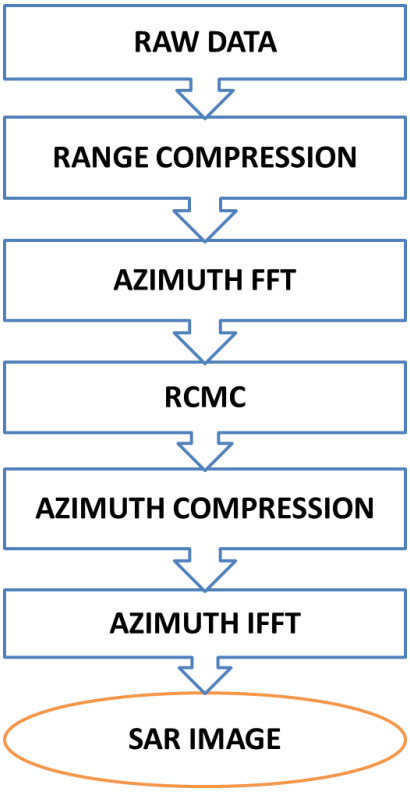

Figure 2.7: Basic RDA steps

Azimuth FFT

The purpose of performing an azimuth FFT is to transform the range compressed signal to the range-Doppler domain. Having the signal in the range-Doppler domain aids/simplifies the range cell migration correction as explained in the next section.

Range Cell Migration Correction (RCMC)

Although the radar motion seems a good solution to increasing the radar resolution by creating the effect of a larger aperture, this motion also causes problems in the signal processing such as migration of range cells. RCMC is a technique used to correct Range Cell Migration (RCM). Due to the motion of the platform, the slant

range of a target varies; therefore, a point target could be seen in different resolution cells. RCMC is an interpolation algorithm that corrects this cell 'migration'. For point targets, which are in the same range bin but are separated in azimuth, when transformed to the range-Doppler domain, the energy of each of these targets become collocated. This makes computation easier because the migration can be applied once for all these targets. This highlights one of the advantages of the range Doppler algorithm.

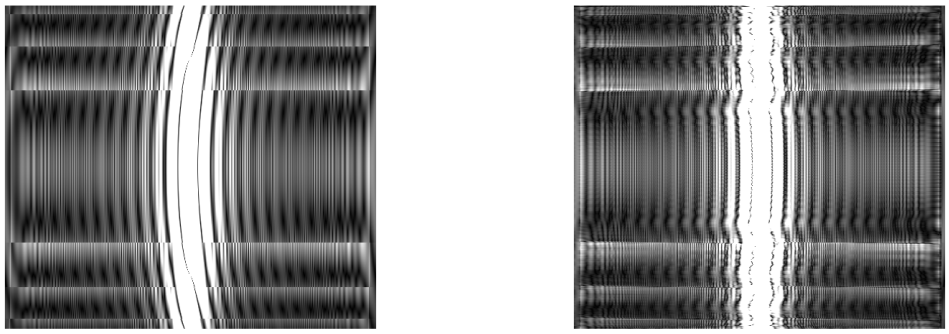

(a) Range compressed data in R-D domain (b) After correction

Figure 2.8: Effect of RCMC

Azimuth compression and Azimuth IFFT

The next step is the azimuth compression, which like the range compression comprises of applying matched filtering to the RCM corrected signal. Since the input signal to this stage is already in the range time and azimuth-frequency domain, there is no need for performing a Fourier transform. The matched filter is just applied to the input signal, which is computationally efficient. After a matched filter is applied, the inverse Fourier transform is then taken to transform the signal back to the time domain both in range and azimuth. The output here is the SAR image.

2.2.2 Other algorithms

Multilook processing is sometimes used to reduce speckle noise after completion of the RDA steps explained above [1]. Other signal processing algorithms have been used to process SAR data, some of which have incorporated certain RDA techniques. Examples of some of these algorithms include the Chirp Scaling Algorithm (CSA), the Omega-K algorithm, SPECAN algorithm and backprojection [1, 13]. The Omega-K algorithm provides effecient and accurate processing in the 2-D frequency domain and it is advantageous in its handling of high squint and wide aperture cases [1]. The CSA is summarized by Cumming and Wong [1] as :

> The Chirp Scaling Algorithm eliminates the interpolation step and processes the data partly in the range Doppler domain and partly in the 2-D frequency domain. In the 2-D frequency domain, the algorithm performs the bulk operations that are assumed to be range independent.

According to Canada Centre for Remote Sensing, Natural Resources Canada [2], the SPECAN algorithm is usually used in the case of scan SAR processing or low resolution radars as opposed to those mentioned above. The algorithm performs the conventional range compression but azimuth compression is achieved by a matched filter multiply, followed by an azimuth FFT; there is no azimuth IFFT in this case, so the algorithm is very efficient. This saving is possible because of the linear FM structure of the received signal [2].

Chapter 3

TARGET AND RADAR MODELLING

Simulations make understanding systems easier and they give an indication into what the model parameters mean and how they affect the system. In general, simulations make improving theories and testing new or developing concepts easier, faster and less expensive. This chapter describes the breakdown of the radar model, how different sections of the radar were modelled, and also covers basic assumptions made during the modelling of the radar system. A key part of the system model is how the target was modelled, which is shown in the following section. Simulation assumptions are provided at the end of this chapter while the results are presented in the next chapter.

3.1 Target modelling

This is one of the major improvements made by this thesis, as well as a very important aspect of this simulation. The simulation allowed a flexible model in terms of target

type and took this as an input to the program alongside the radar parameters. The target/scene is defined by the suer and it plays a major role in the simulation. The target's major parameters are described from the relationship between the transmitted and received signal power by the radar equation as

$$P_r = \frac{P_t G_t}{4\pi R_t^2} \times \frac{\sigma}{4\pi R_r^2} \times A_e \tag{3.1}$$

where P_t is the transmitter power, G_t is the gain of the transmitting antenna, σ represents the RCS, or scattering coefficient, of the target, A_e is effective aperture (area) of the receiving antenna, R_t is distance from the transmitter to the target and R_r is the distance from the target to the receiver. In the case of mono static radars, the transmitter and receiver are either together or closely located in relative terms hence $R_t = R_r$. The σ in the middle term as represented by Skolnik represents the RCS or reflectivity of the target, which can be defined as the measure of the transmitted EM energy intercepted and reflected by the target [15, 6]. When the radar parameters and position of the target are known, this parameter could give an indication of the target; it is the main parameter in the detection of several military targets [6]. This parameter depends on several variables such as the nature of the target, i.e., in terms of material, its orientation and its shape [15]. Due to these variables, it is difficult to define a strict and standard model for the target as there could be different types of objects in a particular scene and their nature, orientations and sizes could differ. For most of the calculations done in the latter parts, the use of point targets was assumed. A point target is a relatively small element on the surface of the earth or imaging surface that reflects a transmitted pulse by a factor determined by its RCS. The range and azimuth resolutions described in Chapter 2

make up a resolution cell, an example of which is shown in Figure 3.1. If two targets are positioned in the same resolution cell of a radar, as explained earlier, it is hard to individually identify them. Such targets are often referred to as unresolved targets. Another scenario would be if a target is so large that it occupies multiple resolution cells of the radar then it is referred to as an extended target. Examples of these can be seen in Figure 3.1.

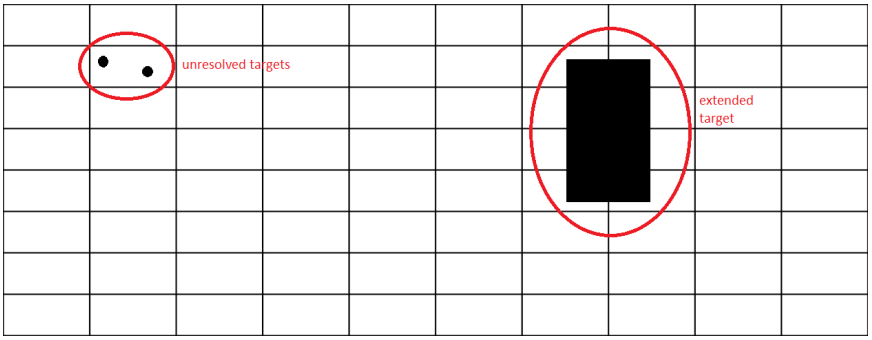

Figure 3.1: Scene showing resolution cells and target types

In this simulation, a scene is considered to contain both point and extended targets with the assumption that the extended targets have uniform reflectivity. This is a very simple assumption and is made due to the fact that a 2-D radar system is being modelled and as stated above, even if the general RCS of the targets in a scene are given, their orientations and sizes could differ wildly thereby changing the RCS values at different points of the target. Due to a 2D image being taken from a high altitude, land vehicles (e.g., a car) could be modelled as a rectangle, a building could take different shapes (square, rectangle, circle, rhombus or a combination of these shapes) and a person, trees and other smaller targets could be modelled as point targets. A particular scene to be imaged could consist of all types of targets, some of which have been mentioned above. The way targets are modelled here is that

they are discretized. The parameter for discretization is the resolution of the radar system. Therefore, if unresolved targets exist, it is nearly impossible for the radar to differentiate between such targets (using only the current information). For an extended target, a function was written to split it into multiple point targets each occupying one resolution cell. For a scene with a cross-sectional area of A', with $A'_{\text{rect}} = L_{\text{scene}} \times W_{\text{scene}}$ for a rectangular scene. Then the number of cells in the scene are represented by

$$N_{\text{cells}} = \frac{A'}{\rho_r \times \rho_a} \tag{3.2}$$

The resolution in both range and azimuth are given by (2.7) and (2.14) respectively. Given a scene with a defined area, the number of resolution cells occupied by the scene is calculated by simply dividing the total area by that of a resolution cell. Due to the scale of the distance of the radar from the scene, $R(\eta)$, and the resolution cells, ρ_r and ρ_a, which is usually in the range of thousands of kilometres vs meters or even centimetres due to pulse compression, each resolution cell could be considered as a point target. Figure 3.1 shows an example of such discretization if the largest rectangle is assumed as the scene of interest, where each small box represents a resolution cell. A simple example will be a radar with a range resolution of 1m and azimuth resolution of 1m i.e., a $1m^2$ resolution cell and a scene area of $400m \times 45m$, maybe containing a ship with a length of $360m$ and beam of $36m$. With the orientation defined, this would result in 400 range bins and 45 azimuth bins resulting in a total of 18,000 resolution cells. With the approach taken in this problem, the scene (an extended target) would be represented by as many point targets as cells, each with a defined position and RCS. It is important to keep in mind that since the RCS of a particular target depends on the orientation, material used and size of the target, each of these

point targets would be replaced with different reflectivity values, depending on the area of a cell occupied by the target. Although according to the assumption of uniform target reflectivity, the cells occupied fully by water will have the same RCS values and so will the cells occupied by the ship due to the uniformity assumed. Areas of the target partially occupying resolution cells are accounted for by multiplying the given target reflectivity by a ratio of the area of the target in that cell by the size of one cell. Examples of this are shown in Chapter 5. The reflectivity used can be represented by

$$\mathrm{A}_{\mathrm{used}} = \alpha_r \times \mathrm{A}_{\mathrm{given}} \tag{3.3}$$

where $\mathrm{A}_{\mathrm{given}}$ represents the given reflectivity of an object in the scene and α_r is a ratio of the target area occupying a cell, $A'_{\mathrm{targetnorm}}$ and the size of a cell, A'_{cell}.

$$\alpha_r = \frac{A'_{\mathrm{targetnorm}}}{A'_{\mathrm{cell}}} \tag{3.4}$$

This section depends on the user, due to infinitely many target scenarios including different types of targets, on different types of ground for example concrete, smooth soil, rough soil, rocks, water, and so on. In the absence of extra geographical information, this method is about as close an estimate that can be given for the target profile.

3.2 Raw data generation - Target Reflections

This section describes the generation of SAR raw data from the input target. As explained in Chapter 2, the 2 dimensional signal is obtained as a result of reflections from the targets back to the radar receiver at different azimuth times. Every point

scatterer reflects EM waves transmitted toward it. As a result of the motion of the platform, a single point target would have multiple reflections stored in memory, each at discrete azimuth times. The total number of reflections depends on the pulse repetition frequency (PRF) of the SAR system and time taken to cover the synthetic aperture and it is in fact the product of both factors. This section is modelled after (2.10) with A_0 and $R(\eta)$ obtained from the target model, $w_r(\tau)$ a simple rectangular square function and $w_a(\eta)$ a sinc-squared function as shown in Section 2.1.2. The use of windows is important in this segment to control the effects of sidelobes. Windows smooth a spectrum by weighing the peak of the spectrum more than its edges. This often affects the resolution of the radar, in fact a wider window worsens the resolution, therefore a balance has to be found between the broadening factor of the window and the resolution of the radar. In this section, both a Hanning window and kaiser windows were used. Although this segment of the simulation seems relatively straight forward because of the equations, it is the most time consuming section of the simulation. This is due to the fact that for each point target, (PRF $\times$ total flight duration) number of reflections are generated and depending on the area of the target profile, there could be multiple point targets obtained from it. For example a simulation with azimuth sampling frequency (PRF) of 100 and 6 seconds flight duration imaging a ship in an ocean covering an area of $13,000m^2$, if the radar's resolution cell is $1m \times 1m$, that would mean generating 600 reflections from 13000 'point' targets. This becomes computationally demanding as the radar resolution increases and the target area increases.

It is important to note that the data collected from this stage is not an image, but in fact data containing information about the transmitted signal, the target reflections

and the motion of the radar platform.

3.3 RDA

The range-Doppler algorithm in the simulation followed the model in Section 2.2.1. The first step, which is the range compression, was modelled by first performing a range Fourier transform on the signal then applying matched filtering, which becomes a multiplication by FT of the complex conjugate of the time reversed pulse signal (the same as that used during the raw data generation). The result obtained is the output of the matched filter but in the frequency domain. An inverse Fourier transform is then applied to transform this signal back to the range time domain because RDA is carried out in the "range time - azimuth frequency" domain. Range FFT in this step was for computational efficiency of matched filtering. The complex conjugate of the time reversed pulse is of the form

$$s(t) = \text{rect}(\frac{t}{T})\exp\{j\pi Kt^2\} \tag{3.5}$$

which is similar to (2.1) when the centre frequency, f_0 , is set to zero [1]. The steps resulting in the range compressed signal (3.8) are shown by the series of equations below.

The raw data in (2.10) is copied below (for convenience)

$$s(\tau,\eta) = \text{A}w_r(\tau - \frac{2R(\eta)}{c})w_a(\eta-\eta_c) \times \exp(-j4\pi f_0\frac{R(\eta)}{c}) \times \exp\{j\pi K_r(\tau - \frac{2R(\eta)}{c})^2\} \tag{3.6}$$

Applying a matched filter of the form

$$h(\tau) = \text{rect}(\frac{\tau}{T})\exp\{-j\pi K\tau^2\} \tag{3.7}$$

which is the time reversed conjugate of $s(t)|_{t=\tau}$ from (2.1)
Time domain convolution of the raw data and matched filter in the range direction yields the pulsed compressed signal

$$s_{rc}(\tau,\eta) = \text{A}p_r(\tau - \frac{2R(\eta)}{c})w_a(\eta-\eta_c) \times \exp(-j4\pi f_0\frac{R(\eta)}{c}) \tag{3.8}$$

An azimuth Fourier transform is then performed on the range compressed signal to obtain a signal in the range-time azimuth-frequency domain, which makes RCMC in the following step more convenient. This transformation is done by using the principle of stationary phase to convert between time and frequency domain and also under the condition that the distance covered by the platform is considerably smaller than the range of closest approach. The next set of equations show how the raw data is obtained in range-Doppler domain. It starts by explaining the phase modulation of the signal as a result of the platform motion.

Due to the condition stated above ($R_0 >> X$, under low squint conditions), R_0 can be approximated by

$$R(\eta) \approx R_0 + \frac{X^2}{2R_0} \tag{3.9}$$

using Taylor series.

By substituting (3.9) in (3.8), the range compressed signal becomes

$$s_{rc}(\tau,\eta) \approx \mathrm{A}p_r(\tau - \frac{2R(\eta)}{c})w_a(\eta-\eta_c) \times \exp\{-j4\pi f_0\frac{R_0}{c}\} \times \exp\{-j\pi\frac{2V_r^2\eta^2}{\lambda R_0}\} \quad (3.10)$$

If compared to (2.10), then the phase modulation in azimuth time can be seen with the linear FM rate here being

$$K_a \approx \frac{2V_r^2}{\lambda R_0} \quad (3.11)$$

from the principle of stationary phase, the relation between azimuth frequency and azimuth time is shown as $f_\eta = -K_a\eta$. Therefore, changing the range compressed signal into the range time azimuth frequency domain, it becomes

$$S_{RD}(\tau,f_\eta) = \mathrm{A}p_r(\tau - \frac{2R_{rd}(f_\eta)}{c})W_a(f_\eta - f_{\eta c}) \times \exp\{-j\frac{4\pi f_0 R_0}{c}\} \times \exp\{j\pi\frac{f_\eta^2}{K_a}\} \quad (3.12)$$

where $W_a(f_\eta - f_{\eta c})$ is the range Doppler equivalent of $w_a(\eta - \eta_c)$

From (3.12), the range is expressed in the range Doppler domain. If in (3.9), the azimuth time is replaced by azimuth frequency using the relationship stated above, then the range in the range Doppler domain can be defined as

$$R_{rd}(f_\eta) \approx R_0 + \frac{V_r^2}{2R_0}(\frac{f_\eta}{K_a})^2, \quad (3.13)$$

but from (3.11), $K_a \approx \frac{2V_r^2}{\lambda R_0}$.

Therefore,

$$R_{rd}(f_\eta) \approx R_0 + \frac{\lambda^2 R_0 f_\eta^2}{8V_r^2} \quad (3.14)$$

Since the desired range should be R_0 at all points as shown in Figure 2.6, the amount of cell migration is given by the additional expression in (3.14) and is denoted by $\Delta R(f_\eta)$

$$\Delta R(f_\eta) = \frac{\lambda^2 R_0 f_\eta^2}{8V_r^2} \tag{3.15}$$

This is then followed by the range cell migration correction. In order to perform this correction, the amount of migration has to be determined, this was determined from (3.15) and can be represented in slow time domain as

$$\Delta R(\eta) = \frac{\lambda^2 R_0 K_a^2 \eta^2}{8V_r^2} \tag{3.16}$$

During the simulation, the range vector is shifted by this factor at corresponding azimuth time steps to give an RCMC range-Doppler version of the initial raw data generated by the radar, $S'_{RD}(\tau, f_\eta)$. After the range cell migration is corrected, azimuth compression is performed in similar fashion to range compression. This time though a direct multiplication can be done since the signal is still in the range Doppler domain. After this is completed, an inverse Fourier transform is performed to change the signal back to the time domain in both directions.

$$S'(\tau, \eta) = \mathrm{IFFT}_\eta\{S'_{RD}(\tau, f_\eta)\} \tag{3.17}$$

The completion of these steps also means the production of a SAR image; all the energy from a point target is now focused to a single point. The simulation results are shown in the next chapter.

3.4 Error model

3.4.1 Model and simulation assumptions

The simulation was based on a model with certain assumptions, some of which are addressed below. First of all, the simulation assumed extended targets have a uniform RCS, and thus they can be broken down into multiple point targets. Another assumption is the use of an airplane as the radar platform. Air vehicles or satellites could be used to carry the radar over the synthesized aperture. The use of an airplane here means the rotation of the earth can be ignored so that for a certain scene (for example, Figure 2.4), the geometry does not change [1]. If a satellite is used, the speed of the platform would have to be considered differently from that of the beam. It was also assumed that the antenna is stationary between transmission and reception of the pulse due to the relatively small distance between the ranges involved [1], i.e., the distance between R_1 or R_2 and consecutive sensor locations from Figure 2.1. Finally, for the usage of RDA, a low squint angle was assumed. Squint angle is the angle between the slant range and the range of closest approach or the range between the transmitted wave and the normal to the azimuth plane [16, 1].

Chapter 4

SIMULATION RESULTS

This section shows the results of the simulation based on the models described in Chapter 3. The first section of this chapter shows the results of point target simulation; the results of a single scatterer and also the output of an attempt to simulate unresolved targets. The next section shows the results of having extended targets in a scene. The result of this is shown from the target information to the discretization by cells and then the resulting SAR image.

4.1 Point targets

The result of simulating a point target located at the centre of a scene is shown in Figure 4.1. The maximum RCS possible is used to allow the point to be visible in the final image. Figure 4.2 shows a zoomed in version in which spectral leakage can be seen. Figure 4.3 shows the image of a scene with two point targets adequately spaced, that is, greater than the radar range resolution both with the same reflectivity values. Again, the spectral leakage can be seen in Figure 4.3. The last figure in this section,

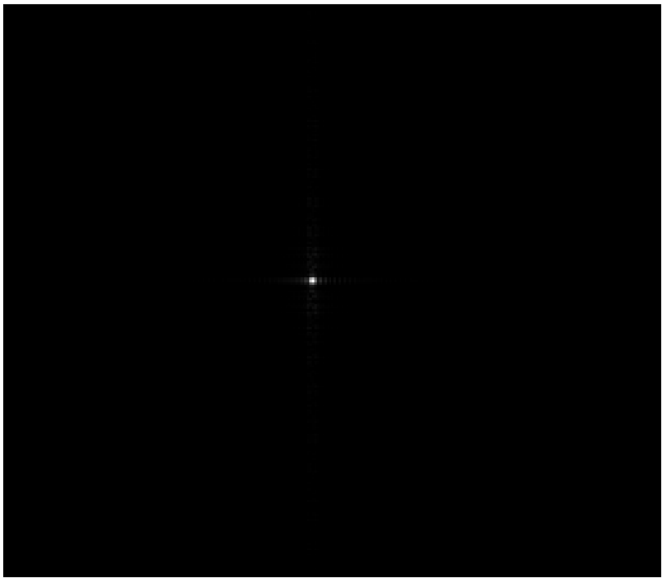

Figure 4.1: Output SAR image from a single point target

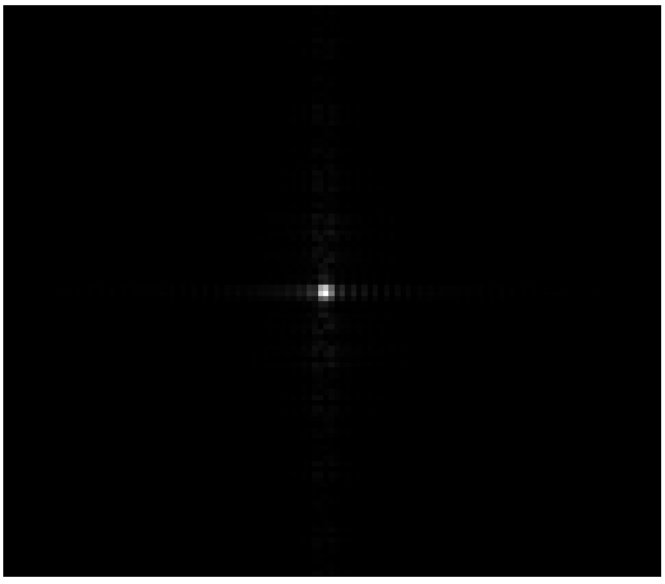

Figure 4.2: Zoomed in image of point target

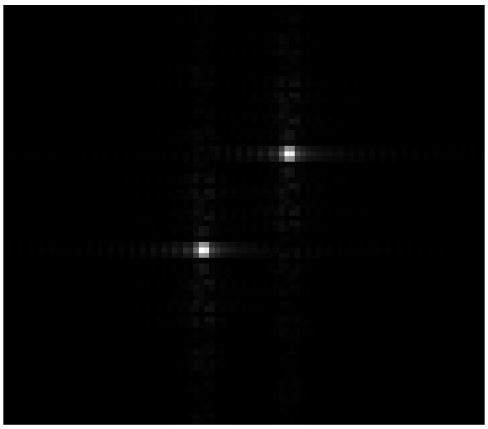

Figure 4.3: Two point targets spaced at a distance larger than resolution

Figure 4.4 shows the result of unresolved targets, in which, both input targets cannot be differentiated and in fact, a false target at an incorrect position is created.

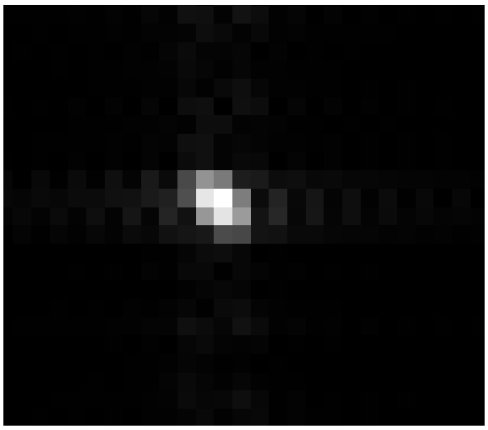

Figure 4.4: Two point targets spaced at a distance less than resolution

4.2 Extended targets

This section shows the results obtained by running simulations on extended targets. The idea, as explained in the previous chapter, is to discretize the scene using the cells of the radar. From this, a higher resolution image will be produced if the resolution of the radar increases. After the discretization, each cell is treated as a point target with partially filled cells, represented by point reflectors. These reflectors have a reflectivity that is modelled by the ratio of target area in the cell by the size of the cell. The downside to this is that relatively small targets like humans, will have really little reflectivity values, hence making them harder to see in the resulting image

4.2.1 Scene example

In Figure 4.5, a scene is presented with a boat [represented as an oval shape], multiple pedestrians [represented by point targets] and two cars [represented by approximate rectangles]. Since this is a 2-D image, these targets are represented by simple shapes.

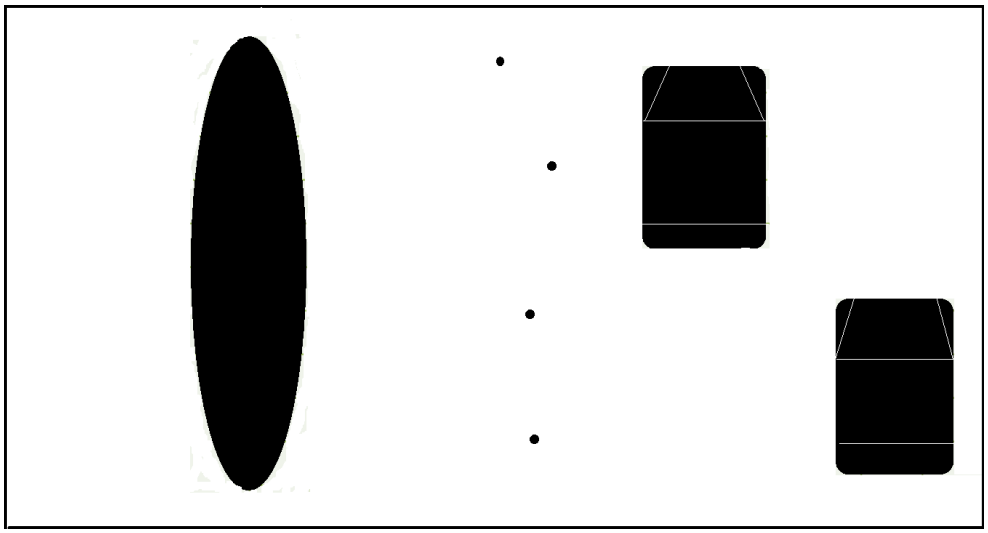

Figure 4.5: Image spread of scene

4.2.2 Target discretization

This section shows the results of target discretization. The radar resolution cells are "placed over" the target scene to split it. The hypothetical image is presented in Figure 4.6, while the corresponding multiple point target matrix is presented in Figure 4.7.

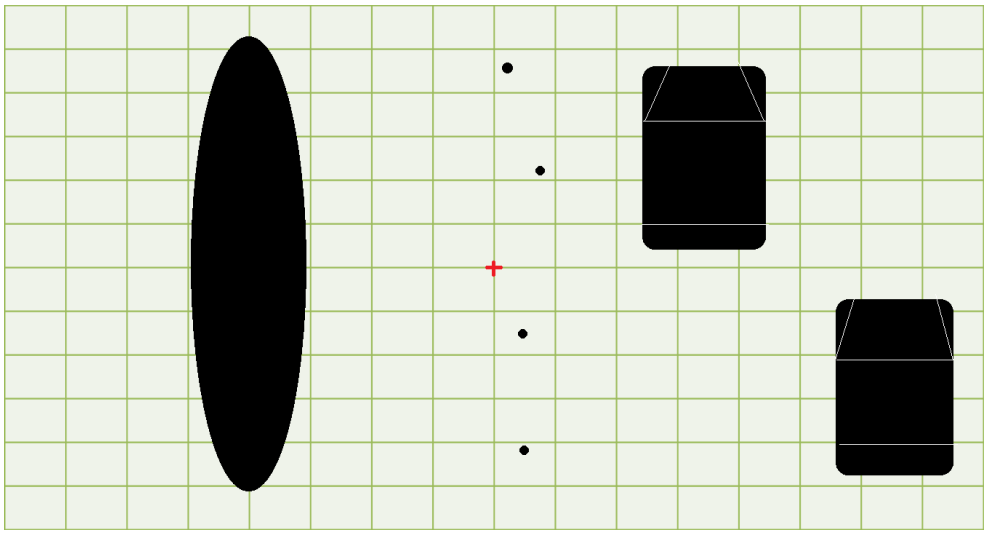

Figure 4.6: Discretized scene

```
sample_scene
[0, 0, 0, 0.1, 0.1, 0, 0, 0, 0, 0, 0, 0, 0, 0, 0, 0, 0;
  0, 0, 0, 0.4, 0.4, 0, 0, 0, 0.1, 0, 0.4, 1, 0.4, 0, 0, 0, 0;
  0, 0, 0, 0.6, 0.6, 0, 0, 0, 0, 0, 0.6, 1, 0.6, 0, 0, 0, 0;
  0, 0, 0, 0.8, 0.8, 0, 0, 0, 0.1, 0, 0.6, 1, 0.6, 0, 0, 0, 0;
  0, 0, 0, 1, 1, 0, 0, 0, 0, 0, 0.6, 1, 0.6, 0, 0, 0, 0;
  0, 0, 0, 1, 1, 0, 0, 0, 0, 0, 0.4, 1, 0.4, 0, 0, 0, 0;
  0, 0, 0, 1, 1, 0, 0, 0, 0, 0, 0, 0, 0, 0.4, 1, 0.4, 0;
  0, 0, 0, 1, 1, 0, 0, 0, 0.1, 0, 0, 0, 0, 0.6, 1, 0.6, 0;
  0, 0, 0, 0.8, 0.8, 0, 0, 0, 0, 0, 0, 0, 0, 0.6, 1, 0.6, 0;
  0, 0, 0, 0.6, 0.6, 0, 0, 0, 0, 0, 0, 0, 0, 0.6, 1, 0.6, 0;
  0, 0, 0, 0.4, 0.4, 0, 0, 0, 0.1, 0, 0, 0, 0, 0.4, 1, 0.4, 0;
  0, 0, 0, 0.1, 0.1, 0, 0, 0, 0, 0, 0, 0, 0, 0, 0, 0, 0;
  0, 0, 0, 0, 0, 0, 0, 0, 0, 0, 0, 0, 0, 0, 0, 0, 0]
```

Figure 4.7: Target matrix as input for raw data generation

4.2.3 SAR image

Figure 4.8 shows the final SAR image of the scene presented in Figure 4.5 given the target matrix in Figure 4.7.

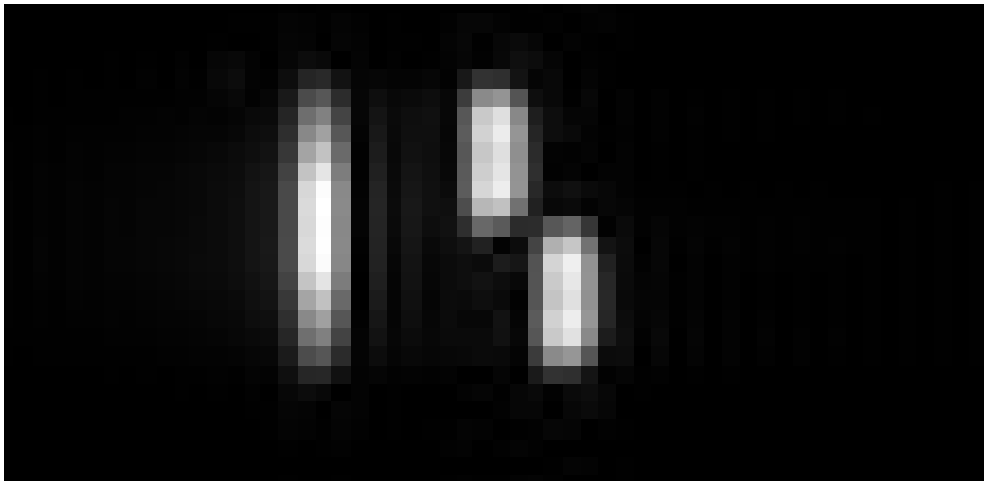

Figure 4.8: FINAL SAR image

As seen in the image above, there still exists some spectral leakage. This is due to not being able to completely eliminate the sidelobes. Also, as the resolution of the radar increases, the output image becomes more accurate because the point target approximation becomes better that is, smaller cells hence, sharper images.

4.3 Comparison

This section compares point target simulations with the model presented by Schlutz [20] and shows the processing time for different number of point targets under the same conditions. Also shown are the simulation parameters, which were used in his simulation and replicated here in order to run the simulation.

Table 4.1: Processing time comparison

no. of targets	previous run time(s)	current run time(s)
1	4.6494	3.75
2	5.22	4.38
4	8.4305	4.84
16	27.7650	13.66
64	111.6868	46.13
256	463.1509	157.37

The simulation parameters below are those from Schlutz's paper, which are used for validating point target results and comparison.

Table 4.2: Simulation parameters used

Parameter	value
azimuth sampling rate (PRF)	300Hz
platform time of flight	3s
aperture length	3m
centre frequency	4.5GHz
platform speed	$200\frac{\text{m}}{\text{s}}$
chirp pulse durations	0.25×10^{-5}s
Bandwidth (or use range sampling rate)	100×10^{6}Hz

Chapter 5

CONCLUSION

This paper explains the core concepts of a synthetic aperture radar, its modes of operations, target and radar model for both point and extended targets as well as the simulation results.

5.1 Conclusion

The concepts of synthesizing the aperture of a radar to produce high quality images are relayed earlier on while the models used for different aspects of the radar are described in the subsequent chapters. The results show the purpose of each step in the simulation, and also show the effects of certain important radar parameters. A model for point targets was presented and simulated by using equations relayed by Cumming and Wong [1] and a new model for handling extended targets was proposed in this paper. This model includes the discretization of the scene by using the resolution cell of the radar. The thesis also shows an improved processing speed by more than 2.5 times from previous models. Modelling extended targets with multiple

point scatterers is not ideal and avoids cases involving scenes with multiple high reflectors that could cause multi-path problems. Another problem that is avoided due to the presented model includes shadowing as a result of oddly shaped targets covering a part of the scene. An increase in speed on previous models seen in the literature review was also achieved by running the simulation in C++ programming language with the aid of OpenCV.

5.2 Further work

There are various aspects in which the different models and simulation can be taken forward. The first includes relaxing some model and simulation assumptions. Certain assumptions (like those discussed in Section 3.4.1) were made, in order to make the model less complicated; these assumptions though were made within reason. Some of these assumptions could be relaxed to make the simulation more realistic and adaptable to different scenarios. For example, the target model was assumed to have uniform reflectivity. In a real scenario, targets are not all uniformly shaped or positioned 'perfectly', neither is the reflectivity uniform. Also, for the simulation it was assumed that the platform carrying the radar is an airplane; an option of a satellite could also be added. The most time consuming part of the simulation is the echo generation. More efficient solutions such as parallel processing/ GPU programming can be implemented in order to reduce the processing time. Also, other SAR processing algorithms could be considered in order to compare and enhance efficiency levels, and also to reduce computational difficulty. After the implementation of the suggestions above, it would be useful to consider a 3-D model to better increase details in the SAR images, making it possible to also account for unresolved targets

with the use of Doppler shifts. Lastly, cases where the target is mobile can then be considered so as to enhance moving target tracking.

Appendix A

PROGRAMMING AND NOTES

A.1 Simulation software

As aforementioned, simulations were done in C++ programming language with the aid of OpenCV library. OpenCV library is an open source C/C++ library with computer vision functions that run on Windows, Mac and Linux OS environments. Several examples from the books by Bradski and Kaehler [21] and Laganière [22] have been used either directly or modified in one way or the other throughout the course of this project to achieve desired math or image processing functions.
The simulation steps include

1. Import the radar parameters from an XML file to instantiate a SAR class
2. Calculate the radar resolution (and other dependent variables) from the given parameters
3. Discretize the scene using the radar resolution and provided scene information

4. Assign reflectivity values to the point target in each cell

5. Generate reflections from every point target and store each reflection (at every azimuth time step) in memory

6. Perform the Range Doppler Algorithm (RDA) to obtain an output image

A.2 Notes

Some of the images presented in this thesis paper have been either imported from or inspired by Cumming and Wong [1], Canada Centre for Remote Sensing, Natural Resources Canada [2] or Wolff [10].

Certain equations presented in the body are extracts from point target radar modelling by Cumming and Wong [1] with some extensions.

With regards to the simulation speed, the written program could have been faster, but certain complex functions, which were non-existent in OpenCV, had to be recreated, some of which slow down the processing time when large matrices are used.

An up-chirp was also used during the simulation, that is, a positive K_r. According to Cumming and Wong [1], the direction of this chirp does not affect the quality of the processed image. This was tested and proved to be the case; the results can be seen in [1].

Bibliography

[1] I. G. Cumming and F. Wong, *Digital signal processing of synthetic aperture radar data: algorithms & implementation*, 1st ed. Norwood: Artech House, Incorporated, 2005.

[2] Canada Centre for Remote Sensing Natural Resources Canada, "Sar systems and digital signal processing," 2007.

[3] H.-C. Chen and C. D. McGillem, "Target motion compensation in synthetic aperture radar," *Aerospace and Electronic Systems Magazine, IEEE*, vol. 6, no. 2, pp. 14–18, 1991.

[4] D. J. Difilippo, G. E. Haslam, and W. S. Widnall, "Evaluation of a kalman filter for sar motion compensation," in *Position Location and Navigation Symposium, 1988. Record. Navigation into the 21st Century. IEEE PLANS'88., IEEE*. IEEE, 1988, pp. 259–268.

[5] B. Zaharris, "Two-dimensional synthetic aperture radar imaging and moving target tracking using the range doppler algorithm simulated in matlab: A thesis," Ph.D. dissertation, California Polytechnic State University, 2007.

[6] C. Ozdemir, *Inverse synthetic aperture radar imaging with MATLAB algorithms*, 1st ed. John Wiley & Sons, Inc., 2012, vol. 210.

[7] E. European space agency. (2013) Advanced synthetic aperture radar. [Online]. Available: https://earth.esa.int/handbooks/asar/toc.htm

[8] U. Madhow, *Fundamentals of digital communication.* Cambridge University Press, 2008.

[9] C. Romero, "High resolution simulation of synthetic aperture radar imaging: A thesis," Master's thesis, California Polytechnic State University, 2010.

[10] C. Wolff. (2011) Radar tutorial. [Online]. Available: http://www.radartutorial.eu/index.en.html

[11] I. Cumming and J. Bennett, "Digital processing of seasat sar data," in *Acoustics, Speech, and Signal Processing, IEEE International Conference on ICASSP'79.*, vol. 4. IEEE, 1979, pp. 710–718.

[12] B. Heck and E. Kamen, *Fundamentals of Signals and Systems Using the Web and MATLAB*, 3rd ed. Prentice-Hall, 2006.

[13] A. F. Yegulalp, "Fast backprojection algorithm for synthetic aperture radar," in *Radar Conference, 1999. The Record of the 1999 IEEE.* IEEE, 1999, pp. 60–65.

[14] J. C. Curlander and R. N. McDonough, *Synthetic Aperture Radar- Systems and signal Processing*, 1st ed. New York: John Wiley & Sons, Inc., 1991.

[15] M. Skolnik, *An introduction and overview of radar.* New York: McGraw-Hill, 2008, vol. 3.

[16] D. R. Wehner, *High Resolution Radar*, 2nd ed. Artech House Inc, 1995.

[17] M. Sack, M. Ito, and I. Cumming, "Application of efficient linear fm matched filtering algorithms to synthetic aperture radar processing," *Communications, Radar and Signal Processing, IEE Proceedings F*, vol. 132, no. 1, pp. 45–57, 1985.

[18] J. Fitch, *Synthetic aperture radar*, 1st ed. New York: Springer-Verlag, 1988.

[19] S. Mehrdad, *Synthetic aperture radar signal processing with Matlab algorithms*, 1st ed. Wily-Interscience, 1999.

[20] M. Schlutz, "Synthetic aperture radar imaging simulated in matlab," Master's thesis, California Polytechnic State University, 2009.

[21] G. Bradski and A. Kaehler, *Learning OpenCV: Computer vision with the OpenCV library*. O'Reilly Media, Incorporated, 2008.

[22] R. Laganière, *OpenCV 2 computer vision application programming cookbook*, 1st ed. Birmingham, UK: Packt Publishing Ltd, 2011.